JOURNAL OF THEORETICAL AND APPLIED MECHANICS
49, 3, pp. 859-878, Warsaw 2011

PIEZOELECTRIC CONTROLLED NOISE ATTENUATION OF ENGINEERING SYSTEMS

Stefan Ringwelski, Tommy Luft, Ulrich Gabbert

Otto-von-Guericke University of Magdeburg, Department of Mechanical Engineering, Magdeburg, Germany; e-mail: stefan.ringwelski@ovgu.de; tommy.luft@ovgu.de; ulrich.gabbert@ovgu.de

In the paper, a recently developed overall numerical approach is presented, which is suitable to design smart engineering systems to actively reduce sound radiation. For this reason, piezoelectric patch actuators and sensors are attached to the surface of the structure to control structural vibrations. In the paper, the theoretical background of the design process is briefly presented first. The basis is a combined finite element and boundary element approach. Electromechanical coupled finite elements are applied to model the structure as well as the piezoelectric patches. The finite element method is also used to model fluid domains which are partially or totally bounded by the structure. Boundary elements are used to characterize the unbounded acoustic pressure fields. Then it is shown how control algorithms can be included into the simulation process, which finally results in an overall simulation approach for structural acoustic systems including control. The numerical approach is also verified by measurements. The experimental setup enables measurements of the uncontrolled and controlled radiated sound fields using a microphone array. A comparison between the measured values and those predicted by the proposed coupled finite element-boundary element approach shows good agreement. Finally, it is demonstrated how the approach can be applied to real engineering systems. As an example, noise reduction of a car engine with a smart oil pan is presented. Again, the numerical results of the uncontrolled and controlled behavior are in good agreement with the measurements. It can be concluded that the proposed overall numerical approach can be applied to design real engineering systems, which are able to actively reduce the noise level.

Key words: FEM, BEM, fluid-structure-interaction, piezoelectricity, active control

1. Introduction

In the past few years, considerable attention has been paid to acoustic noise control in automotive engineering. The application of smart structures provides a way to actively reduce unwanted noise. A smart structure is composed of

a set of actuators and sensors, an inactive structure and an electronic device for controlling. Piezoelectric ceramics are widely used as sensors and actuators, mainly because they can easily be bonded on or imbedded into conventional structures and are lightweight. An often used concept for noise reduction is active structural acoustic control (ASAC) (Fuller, 1990). In this concept, actuators are directly attached to the structure in order to reduce sound radiation by changing the dynamic behavior of the structure. Several researchers have studied different control strategies for ASAC. For example, Li and Zhao (2004) investigated ASAC on a rectangular fluid-loaded plate with piezoelectric layers using a velocity feedback control algorithm. In this study, velocity feedback has been proven to be a robust and effective control strategy.

The development and industrial use of smart structures for ASAC purposes require efficient and reliable simulation and design tools. Virtual models are of particular interest in the design process of a product, since they enable the testing of several control strategies and they are required to determine optimal sensor and actuator locations. A simulation of an active structural acoustic system includes modeling of the passive mechanical structure, the piezoelectric actuators and sensors, the interior and exterior fluids as well as the control algorithm. When dealing with a fluid-loaded shell structure these subsystems cannot be modeled separately, because it is well known that the presence of a surrounding fluid significantly influences the vibration behavior of thin-walled structures.

Accurate modeling of active noise and vibration control has become a topic of wide interest. Wang *et al.* (2006) modeled analytically the controlled behavior of plate-like structures. The effect of piezoelectric actuation was introduced in this model through equivalent bending moments.

More complex problems cannot be solved analytically, and it is necessary to use numerical methods. Several numerical techniques such as the finite element method (FEM) and the boundary element method (BEM) are available to predict the behavior of active structural acoustic systems. A virtual model established entirely on the basis of the FEM was suggested by Khan *et al.* (2002). In this work, infinite acoustic elements are applied to construct a two-dimensional model for harmonic analysis. An extension of this work was given by Lefèvre and Gabbert (2005).

Only a few studies deal with coupling of piezoelectric finite elements with acoustic boundary elements. In Kaljević and Saravanos (1997), a coupled FE-BE approach for computing the steady-state response of acoustic cavities bounded by piezoelectric composite shell structures is presented. Lerch *et al.* (1992) proposed a combined FE-FE-BE scheme for the modeling of acoustic

antennas. In both approaches, the FE-BE model and the FE-FE-BE model are applied only to analyze the interaction between the piezoelectric structure and the surrounding fluid, whereas the influence of control is not considered.

In order to successfully employ piezoelectric patches for active noise attenuation, the response of ASAC systems has to be predicted reliably by an overall model including all subsystems. Therefore, we propose a FE-FE-BE formulation in the frequency domain, which allows the modeling of arbitrary shaped structural acoustic systems including the employed control strategy. The construction of the coupled formulation consists of three parts. First, the piezoelectric structure as well as the enclosed and surrounding fluids are modeled. In the next step, the subsystems are coupled to obtain a multi-coupled system. Lastly, the employed control is implemented in the overall model.

In the present approach, the FEM is employed to model the structure and the piezoelectric patches. Finite elements are also applied to model finite fluid domains around the shell structure as well as fluid domains that are partially or totally bounded by the structure, such as cavities. Conforming boundary elements are utilized to characterize the unbounded acoustic pressure field around the shell structure and the finite fluid domains. A coupled FE-FE--BE approach is derived by introducing coupling conditions which describe the fluid-structure and the fluid-fluid interaction. After coupling the subsystems, the control involved is considered. In simulations of active noise suppression, the influence of control is taken into account simply by implementing the corresponding control algorithm in the structural acoustic model. The present study makes use of velocity feedback control to demonstrate how a closed loop model can be simulated (Fuller and Elliot, 1992; Zhang *et al.*, 2008).

In order to evaluate the accuracy of the proposed modeling approach, simulations of a box-shaped shell structure are presented and compared with measurements. Additionally, it is shown how the approach can be applied to automotive applications. As an example, a stripped car engine that consists of a crankcase and an oil pan with surface-mounted piezoelectric actuators and sensors for active noise reduction is analyzed. Some researchers have already studied active noise reduction of a car (Redaelli *et al.*, 2007) and a truck oil pan (Heintze *et al.*, 2008) using distributed piezoelectric actuators. However in these studies, the oil pan was treated separately and no attempt was made to consider interactions between the crankcase and the oil pan.

The paper is organized in the following way. First, the theoretical background of the numerical approach is presented in detail. The applied finite elements and boundary elements for modeling the mechanical, electromechanical and fluid fields as well as their coupling are described. Then it is shown

how control can be included in the overall multi-field model in the frequency domain. Finally, the closed-loop model developed is used to obtain numerical solutions of a box-shaped shell structure and a stripped car engine. In order to validate the performance of the presented approach, the simulation results are compared with experimental data. It can be observed that, in general, the numerical predictions are in good agreement with the experimental results. The paper concludes with a summary and an outlook over ongoing activities.

2. Finite element and boundary element modeling

In the following, all equations are described using a Cartesian x_1, x_2, x_3--coordinate system.

2.1. Finite element model of piezoelectric structures

The coupled electromechanical behavior of piezoelectric materials in low voltage, strain and stress applications can be modeled with sufficient accuracy by means of linearized constitutive equations. In a matrix form using Voigt notation, the constitutive relations are defined as (Pinto Correia, 2002)

$$\boldsymbol{\sigma} = \mathbf{C}\boldsymbol{\varepsilon} - \mathbf{e}^{\top}\boldsymbol{E} \qquad \boldsymbol{D} = \mathbf{e}\boldsymbol{\varepsilon} + \boldsymbol{\kappa}\boldsymbol{E} \tag{2.1}$$

where $\boldsymbol{\sigma}$ denotes the stress vector and $\boldsymbol{D}$ is the vector of dielectric displacements. $\mathbf{C}$ and $\mathbf{e}$ are the elastic stiffness and the piezoelectric matrices, respectively. $\boldsymbol{\kappa}$ is the dielectric matrix at constant strain. The piezoelectric constitutive relations given above have to be used within the weak form of the mechanical equilibrium equations (Verhoosel and Gutierrez, 2009) to derive the electromechanical FE equations of a piezoelectric material by applying a standard Galerkin procedure. The resulting system of coupled algebraic equations can be expressed as

$$\begin{bmatrix} \mathbf{M}_u & \mathbf{0} \\ \mathbf{0} & \mathbf{0} \end{bmatrix} \begin{bmatrix} \ddot{\boldsymbol{u}} \\ \ddot{\boldsymbol{\varphi}} \end{bmatrix} + \begin{bmatrix} \mathbf{C}_u & \mathbf{0} \\ \mathbf{0} & \mathbf{0} \end{bmatrix} \begin{bmatrix} \dot{\boldsymbol{u}} \\ \dot{\boldsymbol{\varphi}} \end{bmatrix} + \begin{bmatrix} \mathbf{K}_u & \mathbf{K}_{u\varphi} \\ \mathbf{K}_{u\varphi}^{\top} & -\mathbf{K}_{\varphi} \end{bmatrix} \begin{bmatrix} \boldsymbol{u} \\ \boldsymbol{\varphi} \end{bmatrix} = \begin{bmatrix} \boldsymbol{f}_u \\ \boldsymbol{f}_{\varphi} \end{bmatrix} \tag{2.2}$$

where $\boldsymbol{u}$ is the vector with the nodal structural displacements and $\boldsymbol{\varphi}$ is the vector with the nodal values of the electric potentials. The matrices $\mathbf{M}_u$, $\mathbf{K}_u$ and $\mathbf{K}_{\varphi}$ are the structural mass, the structural stiffness and the dielectric matrix, respectively. The piezoelectric coupling arises in the piezoelectric coupling matrix $\mathbf{K}_{u\varphi}$. For convenience, a Rayleigh damping is introduced into

the system of equations (2.2) assuming that the damping matrix $\mathbf{C}_u$ is a linear combination of the matrices $\mathbf{M}_u$ and $\mathbf{K}_u$. The external loads are stored in the mechanical load vector $\boldsymbol{f}_u$ and in the electric load vector $\boldsymbol{f}_\varphi$. In the following, it is assumed that the vector $\boldsymbol{u}$ contains the entire nodal displacements of the mechanical structure as well as the piezoelectric actuators and sensors. Applying the Fourier transform to the above system of equations (2.2) leads to an equivalent system of equations in the frequency domain

$$\begin{bmatrix} -\Omega^2\mathbf{M}_u + \mathrm{i}\Omega\mathbf{C}_u + \mathbf{K}_u & \mathbf{K}_{u\varphi} \\ \mathbf{K}_{u\varphi}^{\top} & -\mathbf{K}_\varphi \end{bmatrix} \begin{bmatrix} \widetilde{\boldsymbol{u}} \\ \widetilde{\boldsymbol{\varphi}} \end{bmatrix} = \begin{bmatrix} \widetilde{\boldsymbol{f}}_u \\ \widetilde{\boldsymbol{f}}_\varphi \end{bmatrix} \tag{2.3}$$

where the vectors $\widetilde{\boldsymbol{u}}$ and $\widetilde{\boldsymbol{\varphi}}$ represent the complex amplitudes of structural displacements and electric potentials. Here, Ω is the excitation frequency and i is the imaginary unit.

Based on formulation (2.3), piezoelectric finite elements of multilayered shell-type and volume-type can be derived. For instance, Ringwelski and Gabbert (2010) developed a simple piezoelectric composite Mindlin-type shell element with eight nodes. Here it is assumed that the thickness of the layers is the same at each node. Additionally, it is presumed that the modeled composite laminate plate consists of perfectly bonded layers and the bonds are infinitesimally thin as well as nonshear-deformable. The shell element has five degrees of freedom $u_1, u_2, u_3, \theta_{x2}, \theta_{x1}$ at each node for the elastic behavior and there is one electric potential degree of freedom φ per layer to model the piezoelectric effect. The normal rotation θ_{x3} is considered to be zero. The poling direction of the piezoelectric layers is assumed to be coincident with the thickness direction x_3, which means that the electric field acts only perpendicular to the layers. Moreover, the difference in the electric potential φ is presumed to be constant in each layer of the shell element. The electric field, which varies linearly through the thickness of a piezoelectric layer, causes an in-plane expansion or contraction. This behavior is called the transverse piezoelectric effect. In Marinković *et al.* (2006) it is shown that these assumptions are accurate enough in thin structure applications.

The applied piezoelectric volume elements have one additional electric potential degree of freedom at each node of the element. More details regarding development and implementation can be found in Gabbert *et al.* (2000).

2.2. Finite element model of the acoustic fluid

Computational prediction of noise can be achieved by the FEM as well as the BEM. When dealing with far-field problems the BEM is very efficient. On the other hand, the FEM is more suitable for bounded fluid regions. For this

reason, a classical FE formulation is employed to model the finite fluid domains that are partially or totally bounded by the structure. The development of acoustic FE elements to calculate time harmonic acoustic pressure waves in homogeneous fluids is based on the Helmholtz equation

$$\Delta\widetilde{p} + k^2\widetilde{p} = 0 \tag{2.4}$$

where $\widetilde{p}$ is the complex amplitude of the time harmonic pressure and k is the wave number. In equation (2.4) Δ is the Laplacian operator. The wave number k is given by

$$k = \frac{\Omega}{c} \tag{2.5}$$

where c is the speed of sound in the fluid. As in structural mechanics, the Helmholtz equation can be cast in a weak form to derive mass-like and stiffness-like element matrices. Following a standard FE assembly procedure, the matrix equation of the discretized fluid domain becomes (Ringwelski and Gabbert, 2010)

$$(-\Omega^2\mathbf{M}_p + \mathbf{K}_p)\widetilde{\boldsymbol{p}} = -\mathrm{i}\rho_0\Omega\widetilde{\boldsymbol{f}}_p \tag{2.6}$$

with the acoustic mass matrix $\mathbf{M}_p$, the acoustic stiffness matrix $\mathbf{K}_p$ and the acoustic load vector $\widetilde{\boldsymbol{f}}_p$ due to the prescribed normal velocities $\widetilde{v}_n$. The variable ρ_0 describes the density of the acoustic medium.

2.3. Boundary element model of the acoustic fluid

Boundary elements are utilized instead of infinite acoustic elements to take into account unbounded acoustic pressure fields around the shell structure and around the finite fluid domains. This is due to the fact that infinite elements do not perform sufficiently well when they are located in the near-field. Boundary elements, on the other hand, can be placed at any arbitrary position.

In boundary elements, the acoustic pressure $\widetilde{p}$ and the normal velocity $\widetilde{v}_n$ are the nodal degrees of freedom. They are linked by the directional derivative (Pates *et al.*, 1995)

$$\frac{\partial\widetilde{p}}{\partial\boldsymbol{n}} = -\mathrm{i}\rho_0\Omega\widetilde{v}_n \tag{2.7}$$

where $\boldsymbol{n}$ is the unit normal vector directed outwards from the fluid domain. The development of a BE formulation is based on Helmholtz equation (2.4), which by means of the weighted residual method and Green's identity can be transformed into the following integral equation

$$\int_O \widetilde{p}\frac{\partial G}{\partial\boldsymbol{n}}\,dO + c_p\widetilde{p} = -\mathrm{i}\rho_0\Omega\int_O G\widetilde{v}_n\,dO \tag{2.8}$$

Here G is the fundamental solution to Helmholtz equation (2.4) and c_p is a factor describing the surface angle of the source point located on the boundary of the radiating domain O. To derive a BE formulation for the acoustic fluid, the standard boundary element discretization together with the collocation method are applied to integral equation (2.8). The resulting direct BE matrix equation reads

$$\mathbf{H}\widetilde{\boldsymbol{p}} = -\mathrm{i}\rho_0 \Omega \mathbf{G}\widetilde{\boldsymbol{v}}_n \tag{2.9}$$

where $\mathbf{H}$ and $\mathbf{G}$ are the influence matrices and the vectors $\widetilde{\boldsymbol{p}}$ and $\widetilde{\boldsymbol{v}}_n$ are the nodal values of the acoustic pressure and the normal velocity. As mentioned before, the BEM only has to deal with a two-dimensional surface model, but the influence matrices $\mathbf{H}$ and $\mathbf{G}$ are fully populated and frequency-dependent.

3. Multi-structural acoustic coupling

The dynamic behavior of lightweight structures with interior and exterior fluid loading is considerably affected by the interaction between the subsystems. Especially in the case of thin-walled structures with openings, fluid-structure and fluid-fluid-interactions take place. The purpose of the following section is to present a FE-FE-BE approach to model the multi-coupling that occurs in systems with the fluid-structure and fluid-fluid interfaces.

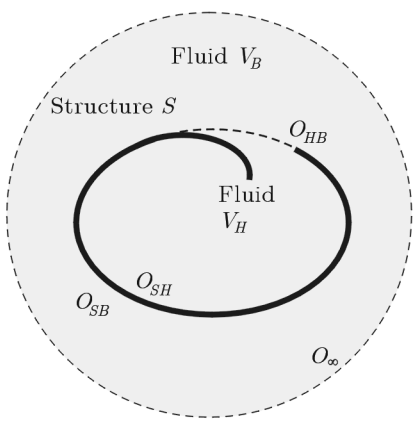

Fig. 1. A multi-coupled structural acoustic system

The approach is illustrated using the multi-coupled structural acoustic system shown in Fig. 1. As illustrated, S is a flexible thin-walled piezoelectric structure that radiates sound into the neighboring fluid domains V_H and V_B.

The fluid domain V_H consists of two parts: an inner region that is substantially enclosed by the structure S, and an outer region that includes sound fields around the openings and acoustic near-fields relevant for controller design purposes. V_B is an unbounded exterior fluid domain surrounding the shell structure S and the finite fluid region V_H.

In the approach, the FEM is applied to model the flexible piezoelectric structure as well as the finite fluid domain V_H. FE modeling of sound fields allows the design of direct acoustic control, since the acoustic pressure is directly available as a nodal degree of freedom, which enables the development of a closed loop model. To predict the harmonic behavior of the unbounded exterior, fluid domain V_B the BEM is applied. A coupled FE-FE-BE formulation is derived by introducing coupling conditions at the fluid-fluid interface O_{HB} and the fluid-structure interfaces O_{SH} and O_{SB}. The coupling conditions are obtained by assuming kinematic and dynamic continuity of structural and acoustic variables at the interfaces. The coupling conditions are given by

$$\begin{aligned} \widetilde{p}_H &= \widetilde{p}_B, & \widetilde{v}_{nH} &= \widetilde{v}_{nB} & &\text{on} & O_{HB} \\ \widetilde{p}_H &= \widetilde{\sigma}_{u_n}, & \widetilde{v}_{nH} &= \mathrm{i}\Omega\widetilde{u}_n & &\text{on} & O_{SH} \\ \widetilde{p}_B &= \widetilde{\sigma}_{u_n}, & \widetilde{v}_{nB} &= \mathrm{i}\Omega\widetilde{u}_n & &\text{on} & O_{SB} \end{aligned} \tag{3.1}$$

At the fluid-fluid interface O_{HB}, the acoustic pressure and the normal particle velocity of the finite and the infinite fluid regions are equal. At the fluid-structure interfaces O_{SB} and O_{SB}, the particles of the fluid and the boundary of the structure move together. As a result, the normal components of the particle velocity and of the first time derivative of the structural displacement are equal, and the acoustic pressure and the normal stress at the surface of the structure are in equilibrium.

Using equation (2.3) and interface relations (3.1), the FE formulation of the fluid-loaded piezoelectric structure S can be written as

$$\begin{bmatrix} \widetilde{\mathbf{K}}_u & \mathbf{K}_{u\varphi} \\ \mathbf{K}_{u\varphi}^{\top} & -\mathbf{K}_{\varphi} \end{bmatrix} \begin{bmatrix} \widetilde{\boldsymbol{u}} \\ \widetilde{\boldsymbol{\varphi}} \end{bmatrix} = \begin{bmatrix} \widetilde{\boldsymbol{f}}_u + \mathbf{L}_{SH}\widetilde{\boldsymbol{p}}_H + \mathbf{L}_{SB}\widetilde{\boldsymbol{p}}_B \\ \widetilde{\boldsymbol{f}}_{\varphi} \end{bmatrix} \tag{3.2}$$

with

$$\widetilde{\mathbf{K}}_u = -\Omega^2\mathbf{M}_u + \mathrm{i}\Omega\mathbf{C}_u + \mathbf{K}_u \tag{3.3}$$

In equation (3.2) there are two additional load vectors describing the sound pressure that acts on the vibrating structure. The matrices $\mathbf{L}_{SH}$ and $\mathbf{L}_{SB}$ are coupling matrices including the shape functions of the structural element and the corresponding hexahedron and boundary element, respectively.

The model of the finite fluid region V_H is based on the equations (2.6) and (3.1). If the vector of the acoustic pressure $\widetilde{\boldsymbol{p}}_H$ in equation (2.6) is split into the inner degrees of freedom $\widetilde{\boldsymbol{p}}_H^V$ and degrees of freedom along the boundaries O_{SH} and O_{HB}, the FE formulation of the finite fluid region can be written as

$$\begin{bmatrix} \widetilde{\mathbf{K}}_p^{11} & \widetilde{\mathbf{K}}_p^{12} & \widetilde{\mathbf{K}}_p^{13} \\ \widetilde{\mathbf{K}}_p^{21} & \widetilde{\mathbf{K}}_p^{22} & \widetilde{\mathbf{K}}_p^{23} \\ \widetilde{\mathbf{K}}_p^{31} & \widetilde{\mathbf{K}}_p^{32} & \widetilde{\mathbf{K}}_p^{33} \end{bmatrix} \begin{bmatrix} \widetilde{\boldsymbol{p}}_H^S \\ \widetilde{\boldsymbol{p}}_H^V \\ \widetilde{\boldsymbol{p}}_H^B \end{bmatrix} = \begin{bmatrix} \rho_0 \Omega^2 \mathbf{L}_{SH}^\top \widetilde{\boldsymbol{u}} \\ \mathbf{0} \\ \mathrm{i}\rho_0 \Omega \mathbf{L}_{HB} \widetilde{\boldsymbol{v}}_{nB} \end{bmatrix} \tag{3.4}$$

with

$$\begin{aligned} \widetilde{\mathbf{K}}_p^{11} &= \Omega^2 \mathbf{M}_p^{11} + \mathbf{K}_p^{11} \\ \widetilde{\mathbf{K}}_p^{12} &= \Omega^2 \mathbf{M}_p^{12} + \mathbf{K}_p^{12} \\ &\vdots \\ \widetilde{\mathbf{K}}_p^{33} &= \Omega^2 \mathbf{M}_p^{33} + \mathbf{K}_p^{33} \end{aligned} \tag{3.5}$$

Due to the load of the mechanical structure and the exterior fluid, there are two additional load vectors. The matrix $\mathbf{L}_{HB}$ is a further coupling matrix which contains the shape functions of the hexahedron and the corresponding boundary element.

In an analogous manner, BE formulation (2.9) can be split into degrees of freedom along the boundary O_{HB} and degrees of freedom along the boundary O_{SB} to predict the behavior of the unbounded exterior fluid domain V_B. The resulting equation reads

$$\begin{bmatrix} \mathbf{H}^{11} & \mathbf{H}^{12} \\ \mathbf{H}^{21} & \mathbf{H}^{22} \end{bmatrix} \begin{bmatrix} \widetilde{\boldsymbol{p}}_B^S \\ \widetilde{\boldsymbol{p}}_H^B \end{bmatrix} = -\mathrm{i}\rho_0 \Omega \begin{bmatrix} \mathbf{G}^{11} & \mathbf{G}^{12} \\ \mathbf{G}^{21} & \mathbf{G}^{22} \end{bmatrix} \begin{bmatrix} \mathrm{i}\Omega \mathbf{T}_{BS} \widetilde{\boldsymbol{u}} \\ \widetilde{\boldsymbol{v}}_{nB}^H \end{bmatrix} \tag{3.6}$$

where the matrix $\mathbf{T}_{BS}$ transforms the nodal displacements of the structural element into the normal velocities of the boundary element.

Combining equations (3.2), (3.4) and (3.6), and moving all unknowns to the left-hand side, the following coupled FE-FE-BE matrix equation is obtained

$$\begin{bmatrix} \widetilde{\mathbf{K}}_u & \mathbf{K}_{u\varphi} & -\mathbf{L}_{SH} & \mathbf{0} & \mathbf{0} & -\mathbf{L}_{SB} & \mathbf{0} \\ \mathbf{K}_{u\varphi}^{\top} & -\mathbf{K}_{\varphi} & \mathbf{0} & \mathbf{0} & \mathbf{0} & \mathbf{0} & \mathbf{0} \\ -\rho_0\Omega^2\mathbf{L}_{SH}^{\top} & \mathbf{0} & \widetilde{\mathbf{K}}_p^{11} & \widetilde{\mathbf{K}}_p^{12} & \widetilde{\mathbf{K}}_p^{13} & \mathbf{0} & \mathbf{0} \\ \mathbf{0} & \mathbf{0} & \widetilde{\mathbf{K}}_p^{21} & \widetilde{\mathbf{K}}_p^{22} & \widetilde{\mathbf{K}}_p^{23} & \mathbf{0} & \mathbf{0} \\ \mathbf{0} & \mathbf{0} & \widetilde{\mathbf{K}}_p^{31} & \widetilde{\mathbf{K}}_p^{32} & \widetilde{\mathbf{K}}_p^{33} & \mathbf{0} & -\mathrm{i}\rho_0\Omega\mathbf{L}_{HB} \\ -\rho_0\Omega^2\mathbf{G}^{11}\mathbf{T}_{BS} & \mathbf{0} & \mathbf{0} & \mathbf{0} & \mathbf{H}^{12} & \mathbf{H}^{11} & \mathrm{i}\rho_0\Omega\mathbf{G}^{12} \\ -\rho_0\Omega^2\mathbf{G}^{21}\mathbf{T}_{BS} & \mathbf{0} & \mathbf{0} & \mathbf{0} & \mathbf{H}^{22} & \mathbf{H}^{21} & \mathrm{i}\rho_0\Omega\mathbf{G}^{22} \end{bmatrix} \begin{bmatrix} \widetilde{\boldsymbol{u}} \\ \widetilde{\boldsymbol{\varphi}} \\ \widetilde{\boldsymbol{p}}_H^S \\ \widetilde{\boldsymbol{p}}_H^V \\ \widetilde{\boldsymbol{p}}_H^B \\ \widetilde{\boldsymbol{p}}_B^S \\ \widetilde{\boldsymbol{v}}_{nB}^H \end{bmatrix} = \begin{bmatrix} \widetilde{\boldsymbol{f}}_u \\ \widetilde{\boldsymbol{f}}_{\varphi} \\ \mathbf{0} \\ \mathbf{0} \\ \mathbf{0} \\ \mathbf{0} \\ \mathbf{0} \end{bmatrix} \tag{3.7}$$

It should be noted that throughout the whole approach conforming meshes are assumed.

4. Velocity feedback control

Analysis of fluid-loaded smart shell structures requires not only the design of an appropriate structural acoustic model but has to take into consideration the control involved as well. In numerical analyses, the influence of control can be taken into account simply by implementing the corresponding control algorithm in the coupled structural acoustic model. The present study makes use of velocity feedback control to demonstrate how a closed loop model can be obtained. Collocated piezoelectric actuators and sensors are utilized to form the closed-loop control system. The collocated design of an actuator/sensor pair guarantees control stability. In the feedback-control system considered, the sensor output voltage is differentiated, amplified by a constant gain g and fed back directly to the collocated actuator. Due to the feedback, the collocated actuator generates counteracting moments which suppress vibrations and the resulting sound radiation of the shell structure. The velocity feedback control law of a collocated actuator/sensor pair reads in the frequency domain

$$\widetilde{\varphi}_a = \mathrm{i}\Omega g\widetilde{\varphi}_s \tag{4.1}$$

where $\widetilde{\varphi}_s$ is the voltage taken from the piezoelectric sensor and $\widetilde{\varphi}_a$ is the voltage applied to the collocated piezoelectric actuator.

Considering a fluid-loaded shell structure with multiple collocated actuator/sensor pairs, the vector of the electric potentials $\widetilde{\boldsymbol{\varphi}}$ in equation (3.7) can be split into degrees of freedom of the sensor layers $\widetilde{\boldsymbol{\varphi}}_s$ and the actuator layers $\widetilde{\boldsymbol{\varphi}}_a$. The control algorithm of multiple independent local feedback loops can be written in the following vector-matrix notation

$$\widetilde{\boldsymbol{\varphi}}_a = \mathrm{i}\Omega \mathbf{G} \widetilde{\boldsymbol{\varphi}}_s \tag{4.2}$$

The control matrix $\mathbf{G}$ in equation (4.2) accomplishes two things. It determines the gains within the local feedback loops and relates the potential degrees of freedom of the sensor layers to those of the corresponding actuator layers. With control algorithm (4.2), the prescribed electric potentials $\widetilde{\boldsymbol{\varphi}}_a$ in the split form of equation (3.7) can be eliminated. The condensed system has the following form

$$\begin{bmatrix}
\widetilde{\mathbf{K}}_u & \mathbf{K}^s_{u\varphi} + \mathrm{i}\Omega \mathbf{K}^a_{u\varphi}\mathbf{G} & -\mathbf{L}_{SH} & \mathbf{0} & \mathbf{0} & -\mathbf{L}_{SB} & \mathbf{0} \\
\mathbf{K}^{s\,\top}_{u\varphi} & -\mathbf{K}^s_{\varphi} & \mathbf{0} & \mathbf{0} & \mathbf{0} & \mathbf{0} & \mathbf{0} \\
-\rho_0\Omega^2\mathbf{L}^{\top}_{SH} & \mathbf{0} & \widetilde{\mathbf{K}}^{11}_p & \widetilde{\mathbf{K}}^{12}_p & \widetilde{\mathbf{K}}^{13}_p & \mathbf{0} & \mathbf{0} \\
\mathbf{0} & \mathbf{0} & \widetilde{\mathbf{K}}^{21}_p & \widetilde{\mathbf{K}}^{22}_p & \widetilde{\mathbf{K}}^{23}_p & \mathbf{0} & \mathbf{0} \\
\mathbf{0} & \mathbf{0} & \widetilde{\mathbf{K}}^{31}_p & \widetilde{\mathbf{K}}^{32}_p & \widetilde{\mathbf{K}}^{33}_p & \mathbf{0} & -\mathrm{i}\rho_0\Omega\mathbf{L}_{HB} \\
-\rho_0\Omega^2\mathbf{G}^{11}\mathbf{T}_{BS} & \mathbf{0} & \mathbf{0} & \mathbf{0} & \mathbf{H}^{12} & \mathbf{H}^{11} & \mathrm{i}\rho_0\Omega\mathbf{G}^{12} \\
-\rho_0\Omega^2\mathbf{G}^{21}\mathbf{T}_{BS} & \mathbf{0} & \mathbf{0} & \mathbf{0} & \mathbf{H}^{22} & \mathbf{H}^{21} & \mathrm{i}\rho_0\Omega\mathbf{G}^{22}
\end{bmatrix} \cdot$$

$$\cdot \begin{bmatrix} \widetilde{\boldsymbol{u}} & \widetilde{\boldsymbol{\varphi}}_s & \widetilde{\boldsymbol{p}}^S_H & \widetilde{\boldsymbol{p}}^V_H & \widetilde{\boldsymbol{p}}^B_H & \widetilde{\boldsymbol{p}}^S_B & \widetilde{\boldsymbol{v}}^H_{nB} \end{bmatrix}^{\top} = \begin{bmatrix} \widetilde{\boldsymbol{f}}_u & \mathbf{0} & \mathbf{0} & \mathbf{0} & \mathbf{0} & \mathbf{0} & \mathbf{0} \end{bmatrix}^{\top} \tag{4.3}$$

Here it is assumed that the actuator/sensor pairs are modeled by independent piezoelectric composite shell elements with one electric potential degree of freedom. As a result, the dielectric matrix $\mathbf{K}_{\varphi}$ becomes diagonal (Li and Zhao, 2004). In addition, it is presumed that for the sensor layer the charge applied $\widetilde{\boldsymbol{f}}^s_{\varphi}$ is zero. In equation (4.3), the subscript a refers to the actuator layers and the subscript s refers to the sensor layers.

The obtained system of equations (4.3) describes the controlled behavior of fluid-loaded smart shell structures. Due to the implementation of a velocity feedback control, an additional damping term occurs on the left-hand side of equation (4.3). The feedback control forces generated by the feedback voltage increase actively the damping of the system. From equation (4.2) it is known that the intensity of the active damping depends on the chosen feedback gains only. Thus, by adjusting the feedback gains, the goal of controlling the vibration and the resulting sound radiation of the shell structure can be achieved.

A drawback of the velocity feedback control is that the sound radiation of the shell structure is not controlled directly, since the control forces are generated to minimize vibration of the structure. Due to the indirect control, the sound pressure in the far-field may not be suppressed as much as the structural

vibration. This is due to the fact that the control applied suppresses not only the vibration but also causes changes in the shape of the vibration modes. Consequently, it is possible that the modified mode shapes produce a higher sound pressure at some points, if the radiated sound waves enhance each other. To overcome the problem, several ASAC strategies have been proposed, such as optimal positioning of the actuator/sensor pairs to minimize the radiated sound power of the vibrating structure (Oude Nijhuis and Boer, 2002).

5. Numerical studies

The purpose of this section is to demonstrate the validity of the proposed modeling approach. For this reason, a number of test simulations are carried out and the results are compared with the experimental data.

5.1. Box-shaped shell structure

As the first test case, a box-shaped shell structure with a partially-enclosed acoustic cavity and an unbounded surrounding fluid domain is considered in the following.

The box-shaped shell structure consists of a thin aluminum plate, four rigid walls and an open side, where the inner and outer fluids interact. The aluminum plate is clamped at all four edges to the rigid walls, which are assumed to be acoustically hard surfaces. Eight piezoceramic patches are bonded on the top and the bottom surfaces of the elastic plate to form a set of four collocated actuator/sensor pairs for active vibration and noise suppression. A velocity feedback control algorithm is applied to relate the sensor voltage to the actuator voltage in four independent feedback loops.

In the approach, the FEM is applied to model the acoustic cavity, and the shell structure, including the rigid walls, the elastic plate as well as the surface-attached piezoelectric actuators and sensors. Each actuator/sensor pair is modeled by a separate independent piezoelectric composite shell element with one potential degree of freedom for each actuator and sensor respectively. A number of 404 standard finite shell elements and 4 piezoelectric composite shell elements are used to model the box-shaped structure. The acoustic cavity is approximated by 832 finite hexahedron elements. The BEM is used to model the exterior sound field. For the unbounded exterior fluid, a conforming discretization with 508 boundary elements is applied. In all these elements,

quadratic serendipity shape functions are employed. For more modeling details see Ringwelski (2011). Figure 2 shows the layout and the mesh used in the numerical modeling.

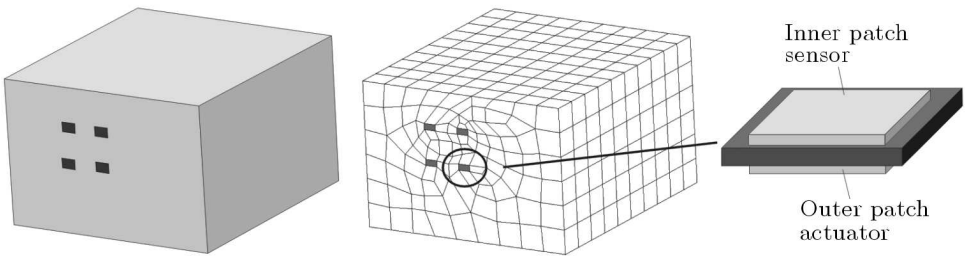

Fig. 2. Layout and conforming FE-FE-BE mesh of the considered fluid-loaded smart shell structure

For comparison between the numerical results and the experiments, steady state acoustic pressure fields of the uncontrolled and controlled system are computed by solving the system of equations (4.3). Figures 3 and 4 illustrate the computed sound pressure distribution over the cross-section of the shell structure. Simulated and measured contour plots are obtained for the case that a harmonic point force of 60 Hz is applied perpendicular to the outer surface of the plate.

In both figures it can be noted that the experimentally measured pressure fields show high consistency with the computed ones. From the good agreement of the results, it can be concluded that the proposed FE-FE-BE formulation allows the modeling of structural acoustic systems in combination with control. Moreover, the figures reveal that for the uncontrolled and controlled case, the sound pressure level inside the acoustic cavity is significantly higher than outside. From the contour plots in Figs. 3 and 4 it can also be seen that due to the controller influence the sound pressure level is reduced by approximately 5 dB. Additionally, the figures demonstrate that the velocity feedback control reduces the response of acoustic pressure locally as well as globally.

The experimental reference solutions were obtained with Hardware-in-the-Loop experiments using a dSPACE controller board which determines the necessary control outputs for the actuators. During the tests, the box-shaped shell structure was placed in an anechoic chamber, which ensures free-field environment. To measure the acoustic pressure, a uniformly distributed microphone-array consisting of 3×7 microphones with a grid spacing of 100 mm was positioned inside the cavity. During the measurements, the microphone array was moved several times to cover the whole cross-section of the box-

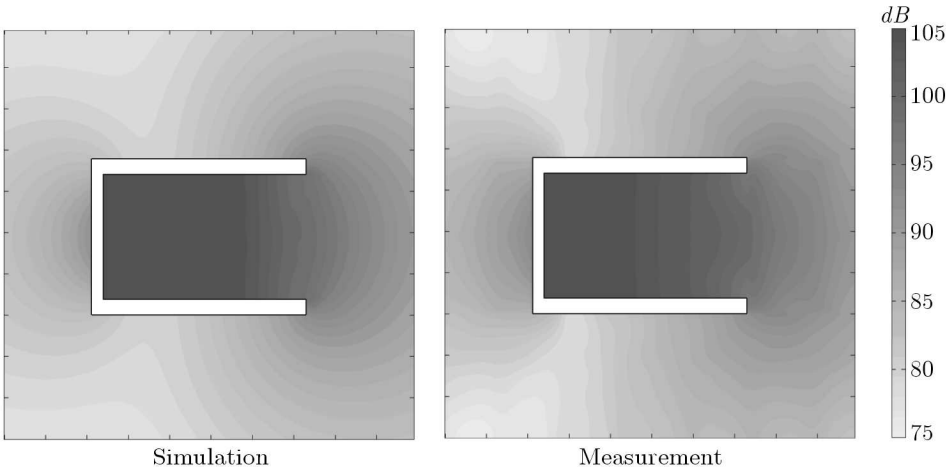

Fig. 3. Sound pressure distribution of the uncontrolled box over the cross-section

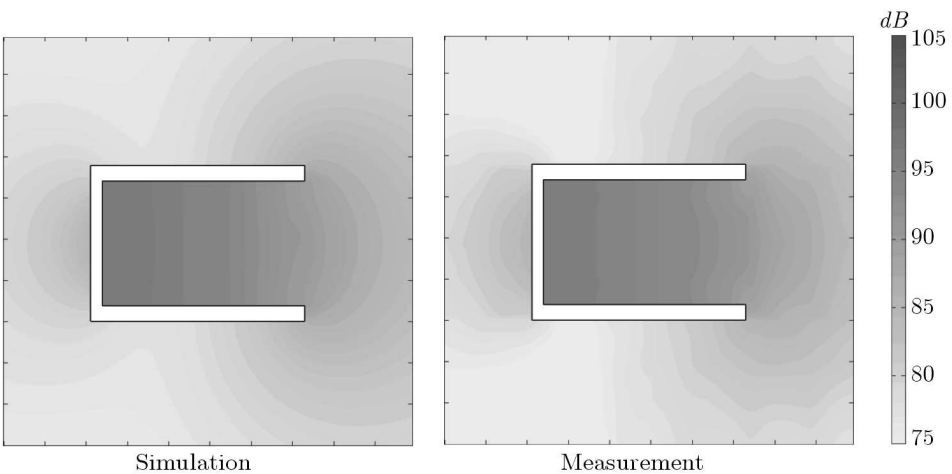

Fig. 4. Sound pressure distribution of the controlled box over the cross-section

shaped shell tructure. More details concerning the experimental testing of the system designed can be found in Ringwelski (2011) and Luft *et al.* (2010).

5.2. Stripped car engine

For further validation, a stripped car engine that consists of a crankcase and an oil pan with surface-mounted piezoelectric actuators and sensors for active noise reduction is analyzed. Two collocated actuator/sensor pairs have

been chosen for active noise reduction. Excitation of the engine is provided by a further actuator placed at the inner side of the oil pan.

Here the actuators and sensors are modeled using 216 6-node multilayer triangular shell elements. A number of 462361 standard finite 10-node tetrahedral elements is used to model the irregular-shaped geometry of the crankcase and the oil pan. The unbounded sound field around the engine is characterized by 4573 8-node boundary elements. Figure 5 illustrates the geometry and the FE mesh of the stripped car engine.

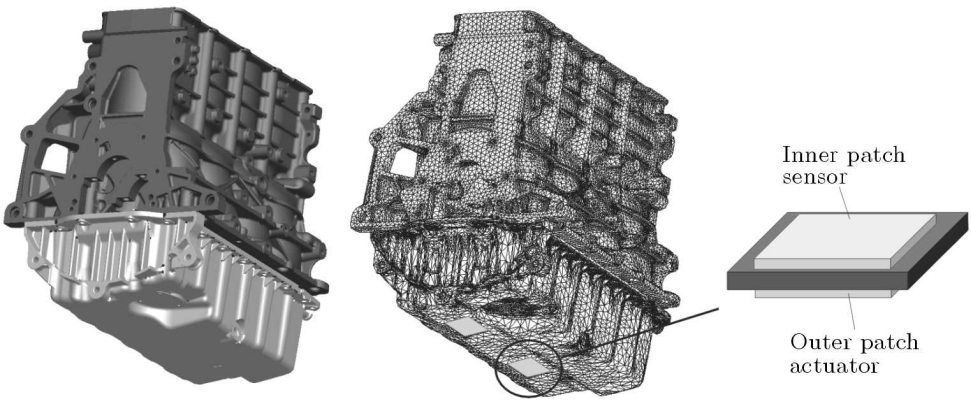

Fig. 5. Layout and conforming FE-FE-BE mesh of the stripped car engine

From the acoustical point of view, the car engine can be treated as a thick-walled structure. This means that the influence of the surrounding air on the structural vibration can be neglected. Additionally, the fluid-fluid interaction does not occur, since there is no further fluid region. Consequently, the acoustical degrees of freedom in equation (4.3) can be decoupled from the rest of the system and calculated in an independent BE simulation after the vibrational behavior of the stripped engine has been computed. For this purpose, the FE calculated structural displacements have to be interpolated onto the grid points of the BE mesh and applied as boundary conditions.

For comparison reasons, steady state acoustic pressure fields of the uncontrolled and controlled engine are computed. In order to obtain a radiated sound field, the first eigenmode of the stripped car engine is excited with the help of the patch actuator placed on the inner side of the smart oil pan. The computed sound pressure distributions are plotted on the left-hand side of Figs. 6 and 7. To verify the simulated data in addition, the corresponding measurements are shown in Figs. 6 and 7. For these measurements, the same experimental setup was used as for the box-shaped shell structure.

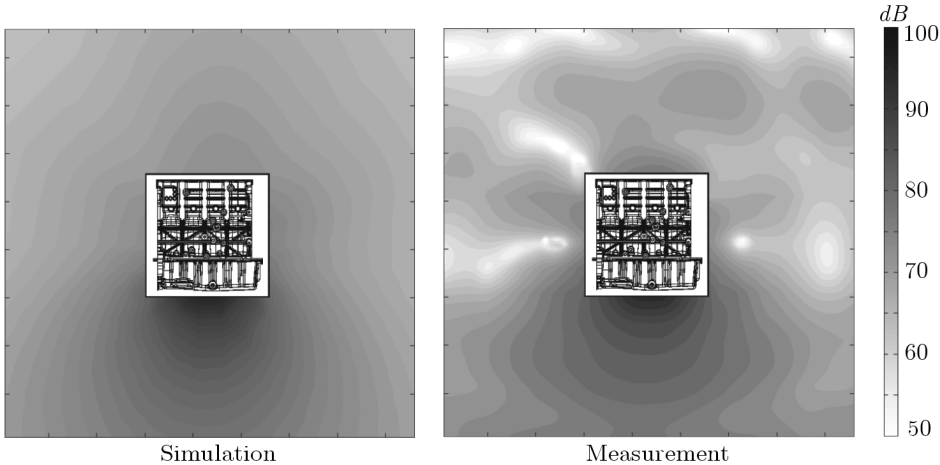

Fig. 6. Sound pressure distribution of the uncontrolled engine over the cross-section

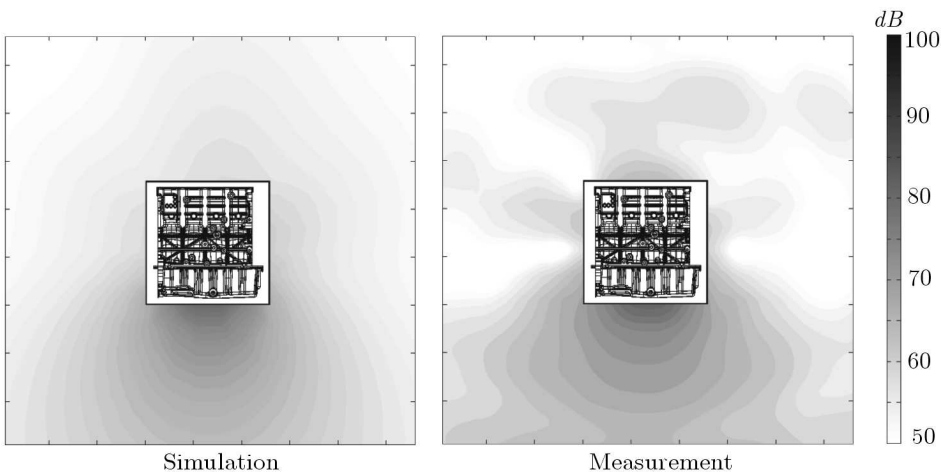

Fig. 7. Sound pressure distribution of the controlled engine over the cross section

It can be noticed that due to the implementation of the velocity feedback control the sound pressure level is reduced by approximately 13 dB, which indicates the noise reduction potential of the designed system. Furthermore, it can be seen that the general trend observed in the simulations and the experimental results is similar. Small differences between measurements and simulations, especially in areas of low sound pressure, are due to the experimental setup. More exact measurements could be achieved if the radiating structure was placed in a more advanced anechoic chamber.

6. Conclusions

In this paper, a coupled FE-FE-BE approach has been presented, which is capable to design engineering systems with surface-mounted piezoelectric actuators and sensors to actively reduce structural vibrations and also sound radiation.

In the approach, the FEM is applied to model the actively controlled piezoelectric structure. The FEM is also employed to predict the behavior of finite fluid domains that are partially or totally bounded by the structure. Boundary elements are used to model the unbounded acoustic pressure fields around the structure and around the finite fluid domains. A procedure has been presented to obtain a FE-FE-BE formulation for modeling the interaction at the fluid-fluid and fluid-structure interfaces. The resulting system of equations has been constructed particularly to simulate the active noise and vibration suppression in the frequency domain. For this reason, it has been shown how the control algorithm can be included into the multi-coupled structural acoustic formulation to provide a closed loop model. In the present study, the velocity feedback control is used to demonstrate the implementation. The presented approach developed is easy to implement in existing FE-BE codes, and there is no restriction regarding the shape of the structure controlled and the control strategy applied.

In order to demonstrate the applicability of the approach developed, a number of test simulations are carried out and the results compared with measurements. As the first test case, a box-shaped shell structure with four collocated actuator/sensor pairs and an open rearward end is considered. It is shown that measured values and those predicted by the coupled FE-FE-BE model are in good agreement. Additionally, the results show that significant damping is achieved due to implementation of the velocity feedback.

Furthermore, it is demonstrated how the approach can be applied to real engineering systems. As a practical example, noise reduction of a smart stripped car engine comprised of a cylinder block and an oil pan with surface-attached piezoelectric actuators and sensors for active noise and vibration reduction is presented. Again the computed pressure fields show a good agreement with those measured and a similar attenuation of sound pressure is obtained.

It can be concluded that the proposed approach is able to model the uncontrolled as well as controlled behavior of fluid-loaded structures with a good quality. Therefore, the present developments provide a powerful basis to model and to design real engineering systems for active noise and vibration suppres-

sion. In relation to ongoing research projects, the performance of the control strategy developed is tested at a diesel engine on a test bench.

Acknowledgements

The work is financially supported by the German Federal State of Saxony-Anhalt and by the European Commission as a part of the research project "COmpetence in MObility". This support is gratefully acknowledged.

References

1. Fuller C.R., 1990, Active control of sound transmission/radiation from elastic plates by vibration inputs. I – Analysis, *Journal of Sound and Vibration*, **136**, 1, 1-15
2. Fuller P.A., Elliott S.J., 1992, *Active Control of Sound*, Academic Press Limited London
3. Gabbert U., Berger H., Köppe H., Cao X., 2000, On modelling and analysis of piezoelectric smart structures by the finite element method, *Journal of Applied Mechanics and Engineering*, **5**, 1, 127-142
4. Heintze O., Misol M., Algermissen S., Hartung C.F., 2008, Active structural acoustic control for a serial production truck oil pan: experimental realization, *Proceedings of the Adaptronic Congress*, Berlin, 147-153
5. Kaljević I., Saravanos D.A., 1997, Steady-state response of acoustic cavities bounded by piezoelectric composite shell structures, *Journal of Sound and Vibration*, **204**, 3, 459-476
6. Khan M.S., Cai C., Hung K.C., Varadan V.K., 2002, Active control of sound around a fluid-loaded plate using multiple piezoelectric elements, *Smart Materials and Structures*, **11**, 346-354
7. Lefèvre J., Gabbert U., 2005, Finite element modelling of vibro-acoustic systems for active noise reduction, *Technische Mechanik*, **25**, 3/4, 241-247
8. Lerch R., Landes H., Friedrich W., Hebel R., Hoss A., Kaarmann H., 1992, Modelling of acoustic antennas with a combined finite-element-boundary-element-method, *Proceedings of the IEEE Ultrasonics Symposium*, 643-654
9. Li S., Zhao D., 2004, Numerical simulation of active control of structural vibration and acoustic radiation of a fluid-loaded laminated plate, *Journal of Sound and Vibration*, **272**, 1/2, 109-124
10. Luft T., Ringwelski S., Gabbert U., Henze W., Tschöke H., 2010, Adaptive controllers for active noise reduction of a stripped engine, *Proceedings of World Automotive Congress*, A-039

11. MARINKOVIĆ D., KÖPPE H., GABBERT U., 2006, Numerically efficient finite element formulation for modeling active composite laminates, *Mechanics of Advanced Materials and Structures*, **13**, 379-392
12. OUDE NIJHUIS M.H.H., BOER DE A., 2002, Finite element models applied in active structural acoustic control, *Proceedings of SPIE*, **4693**, 57-68
13. PATES C.S., SHIRAHATTI U.S., MEI C., Sound-structure interaction analysis of composite panels using coupled boundary and finite element methods, *Journal of the Acoustical Society of America*, **98**, 2, 1216-1221
14. PINTO CORREIA I.F., MOTA SOARES C.M., MOTA SOARES C.A., NORMAM J.H., 2002, Active control of axisymmetric shells with piezoelectric layers: a mixed laminated theory with a high order displacement field, *Computers and Structures*, **80**, 1/2, 2265-2275
15. REDAELLI M., MANZONI S., CIGADA A., WIMMEL R., SIEBALD H., FEHREN H., SCHIEDEWITZ M., WOLFF K., LAHEY H.-P., NUSSMANN C., NEHL J., NAAKE A., 2007, Different techniques for active and passive noise cancellation at powertrain oil pan, *Adaptronic Congress*, Göttingen, 21/1-8
16. RINGWELSKI S., 2011, *Numerische Modelle für die aktive Schwingungs- und Schallereduktion und deren Verifikation*, VDI Fortschritt-Berichte, Reihe 20 Nr. 435, VDI-Verlag GmbH
17. RINGWELSKI S., GABBERT U., 2010, Modeling of a fluid-loaded smart shell structure for active noise and vibration control using a coupled finite element-boundary element approach, *Smart Materials and Structures*, **19**, 10, 105009
18. VERHOOSEL C.V., GUTIERREZ M.A., 2009, Modelling inter- and transgranular fracture in piezoelectric polycrystals, *Engineering Fracture Mechanics*, **76**, 6, 742-760
19. WANG J., SHEPARD JR. W.S., WILLIAMS K.A., GATTIS C.B., 2006, Active vibration control of a plate-like structure with discontinuous boundary conditions, *Smart Materials and Structures*, **15**, 3, N51-N60
20. ZHANG Z., CHEN Y., YIN X., HUA H., 2008, Active vibration isolation and underwater sound radiation control, *Journal of Sound and Vibration*, **318**, 725-736

Tłumienie hałasu w konstrukcjach inżynierskich za pomocą elementów piezoelektrycznych

Streszczenie

W pracy przedstawiono ostatnio opracowaną przez autorów metodę obliczeniową do projektowania konstrukcji „inteligentnych", których zadaniem jest redukcja emisji hałasu. Do samego tłumienia hałasu użyte są elementy piezoelektryczne przyklejane

do powierzchni danej konstrukcji. Na początek omówiono podstawy teoretyczne projektowania takich układów. Podstawę stanowi kombinacja metody elementów skończonych i brzegowych. Elementy skończone ze sprzężeniem elektromechanicznym służą do modelowania piezoelektryków i konstrukcji bazowej. Metodę elementów skończonych zastosowano także do modelowania płynu znajdującego się wewnątrz projektowanego urządzenia przy częściowym lub całkowitym zamknięciu płynu ścianami konstrukcji. Elementy brzegowe użyto do opisu otwartego pola akustycznego. Następnie pokazano sposób, w jaki algorytmy sterowania należy wprowadzić do ogólnej procedury obliczeniowej do projektowania urządzeń z aktywnym układem redukcji hałasu. Otrzymane rezultaty symulacji numerycznych zweryfikowano pomiarami z doświadczeń. Stanowisko badawcze zostało wyposażone w odpowiedni układ mikrofonów, co umożliwiło pomiar poziomu hałasu z włączonym i wyłączonym układem sterowania. Stwierdzono dobrą zgodność wyników eksperymentu z zaproponowaną metodą numeryczną wykorzystującą elementy skończone i brzegowe. Na koniec omówiono przykład zastosowania zaproponowanej metody do projektowania rzeczywistej konstrukcji. Zaprezentowano silnik samochodowy z układem aktywnej redukcji hałasu umiejscowionym na misce olejowej. Powtórnie zbadano zgodność wyników symulacji numerycznych z pomiarami doświadczalnymi, stwierdzając dobrą zgodność pomiędzy nimi. W konkluzji uznano, że zaproponowana metoda nadaje się do zintegrowania z ogólnymi algorytmami projektowania rzeczywistych konstrukcji inżynierskich, w których nacisk położono na redukcję poziomu hałasu.

Manuscript received February 9, 2011; accepted for print April 8, 2011